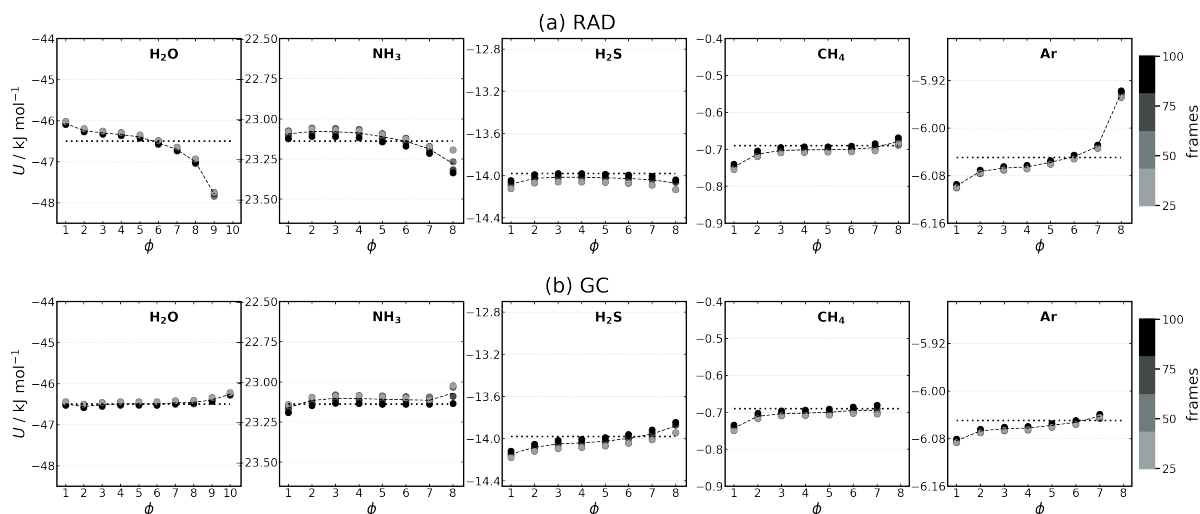


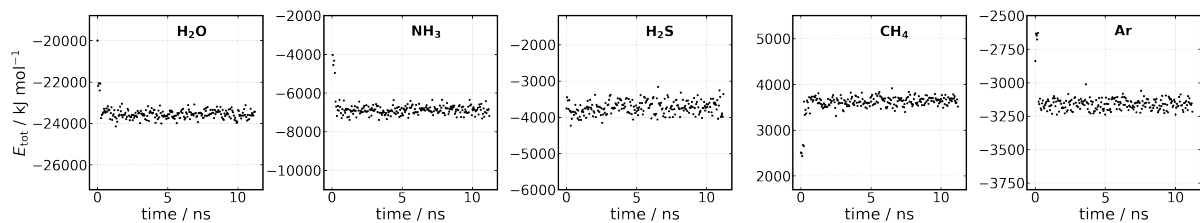
Supplementary Information for "Convergence Behaviour of Solvation Shells in Simulated Liquids"

Jas Kalayan¹ and Richard H. Henchman¹

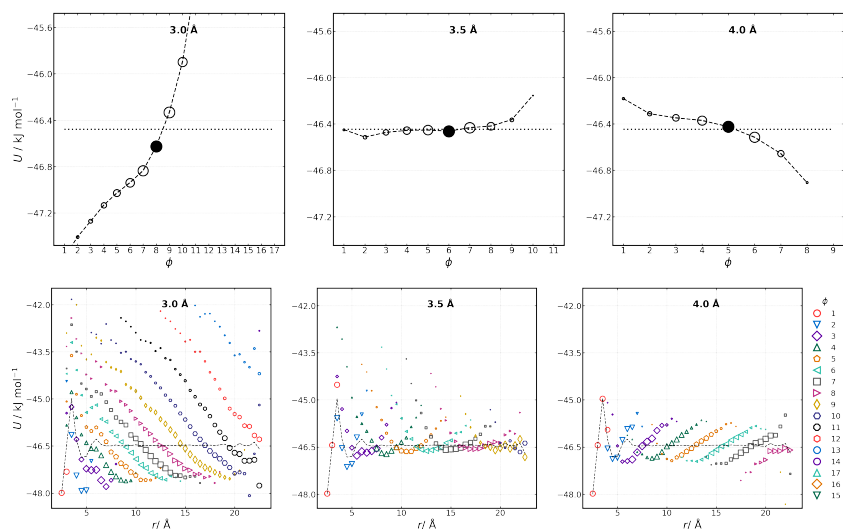
*Manchester Institute of Biotechnology, The University of Manchester, 131 Princess Street, Manchester M1 7DN,
United Kingdom and Department of Chemistry, The University of Manchester, Oxford Road, Manchester M13 9PL,
United Kingdom*



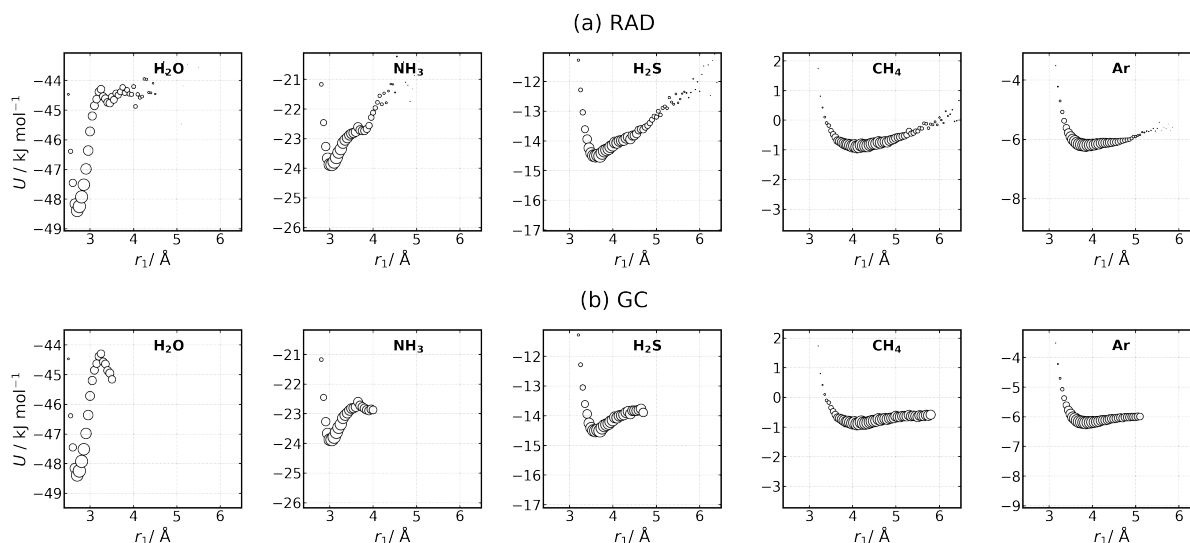
Supplementary Figure S1. Potential energy U per shell shaded by the total number of simulation frames analysed: 25, 50, 75 and 100 frames. U converges across all shells for all liquids, showing that the shell dependence is stable and not a result of insufficient averaging.



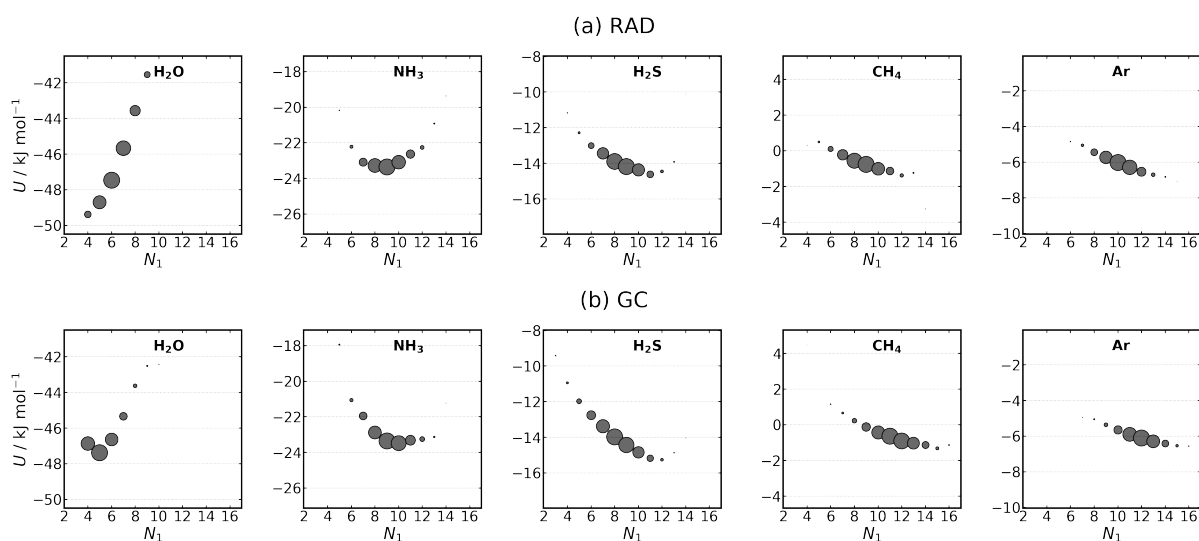
Supplementary Figure S2. Total energy (kinetic plus potential) of systems as a function of simulation time, showing the energy is converged for the final 10 ns for all five liquids over the 100 frames taken for analysis.



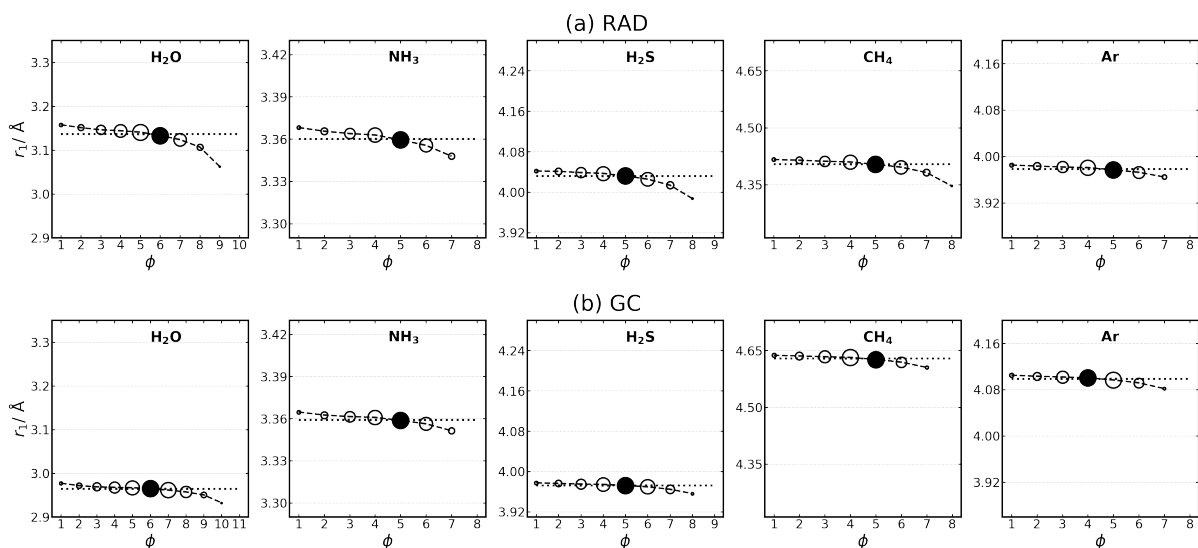
Supplementary Figure S3. Molecular potential energy U versus shell index ϕ (top) for three different GC cutoffs (3, 3.5 and 4 Å) of liquid water, where colored markers represent different distance bins. U versus distance r colored by shell index ϕ (bottom) for the same three GC cutoffs. For both rows, marker sizes represent probability of occurrence. The nature of the dependence of U on ϕ and U distributions within each shell strongly depend on the cutoff used.



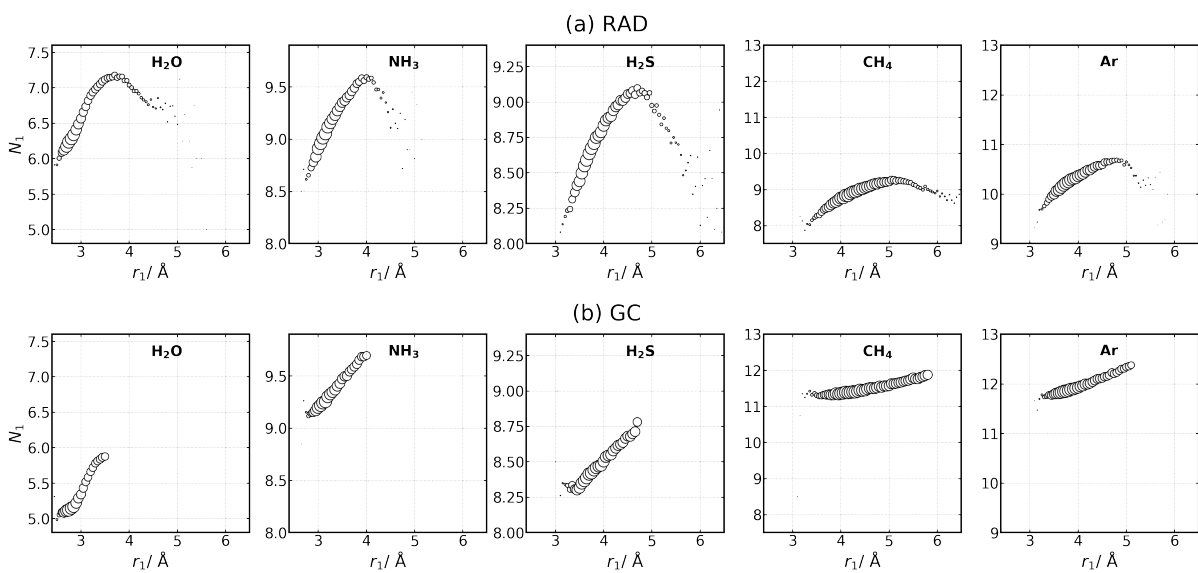
Supplementary Figure S4. Potential energy U versus r_1 using (a) RAD and (b) GC averaged over all shells and with a 0.05 \AA bin width. Circle size represents probability. All liquids show a stable minimum in U at short-range.



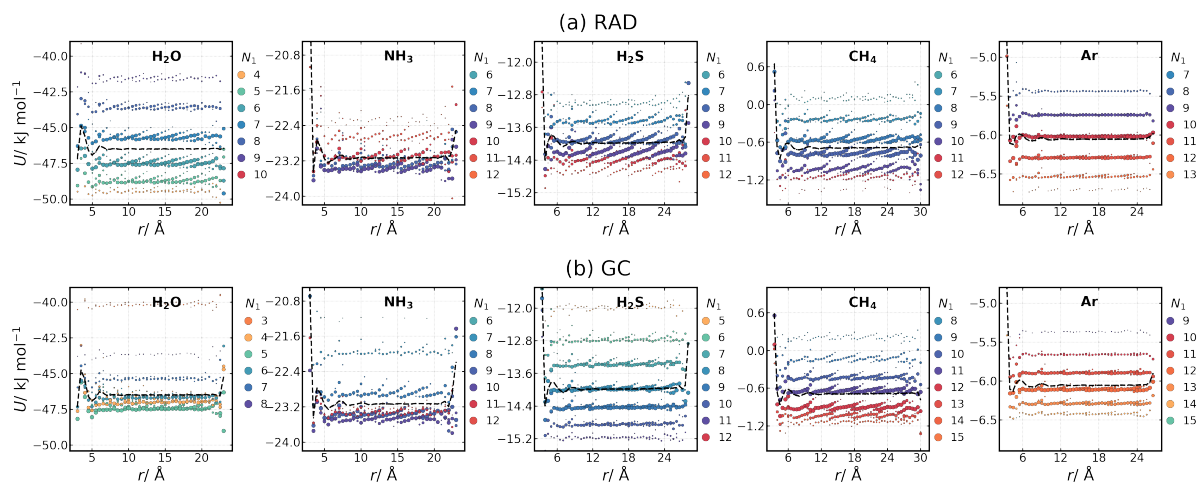
Supplementary Figure S5. Potential energy U versus coordination number N_1 using (a) RAD and (b) GC averaged over all shells. Circle sizes represent probability. The dependence of U depends strongly on the liquid, with non-polar liquids showing an increasing trend and polar liquids showing a decreasing trend.



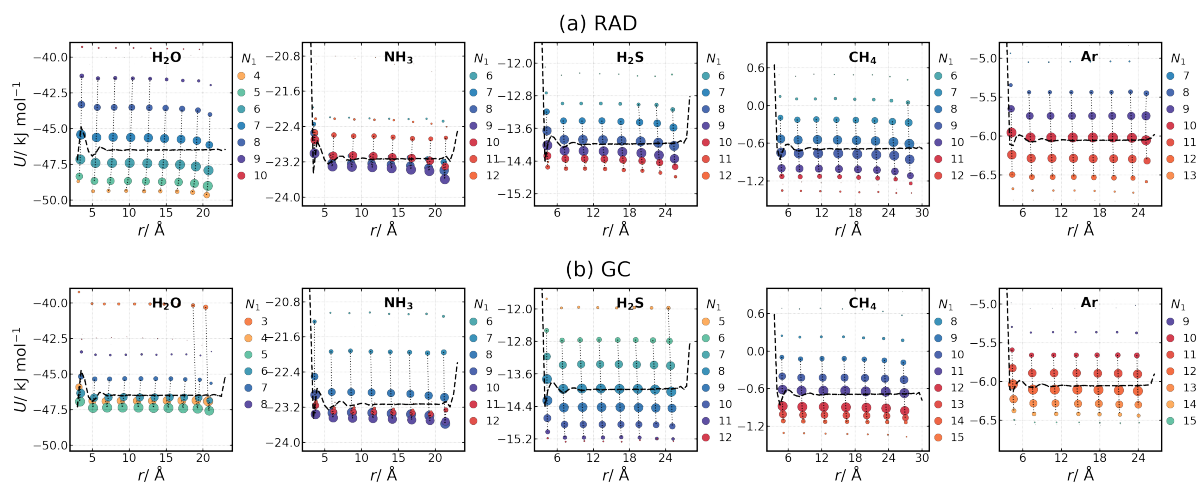
Supplementary Figure S6. Average coordination radii reduce at further shells for all liquids. Average r_1 versus ϕ for each liquid using (a) RAD and (b) GC, together with the r_1 distributions versus r in each shell. The number of molecules in each shell is represented by circle size and the largest shell for each system is filled in black. The value of r_1 decreases with r for all liquids and methods.



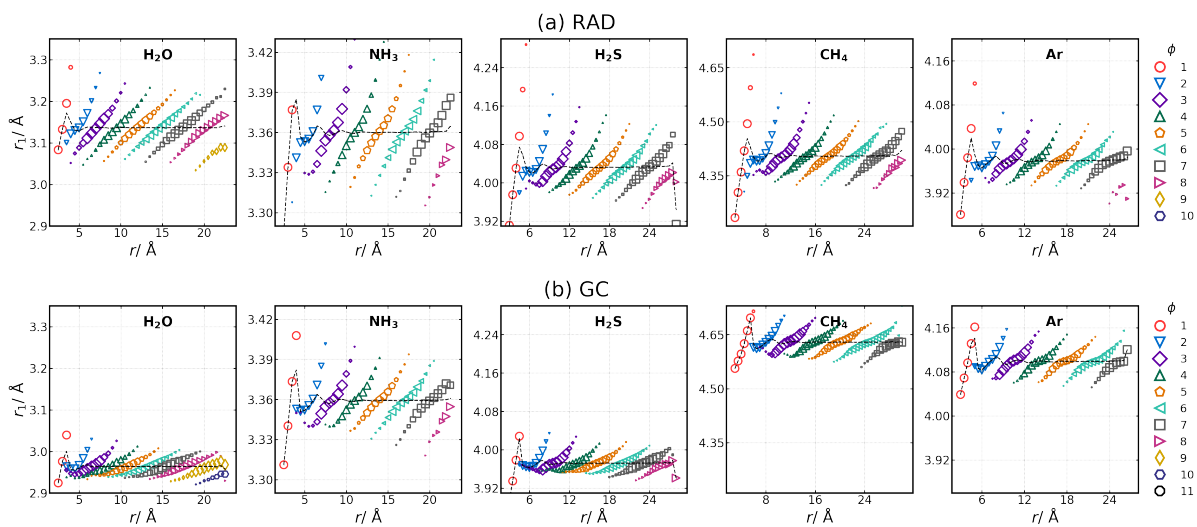
Supplementary Figure S7. Molecule coordination number N_1 versus coordination radius r_1 averaged over all shells using (a) RAD and (b) GC. Larger coordination shell radii result in larger coordination number for all but the highest values of r_1 .



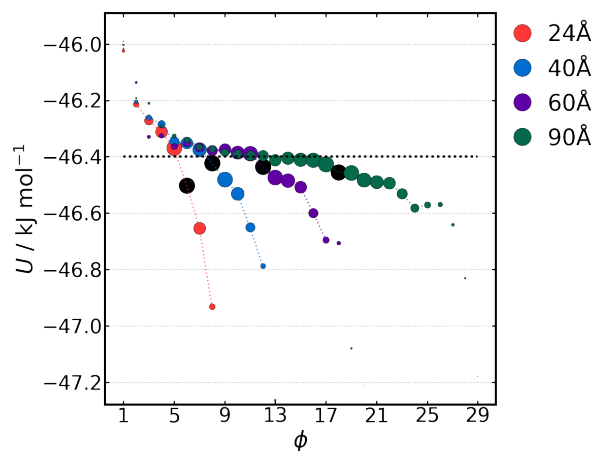
Supplementary Figure S8. Molecular potential energy U versus distance r colored by coordination number N_1 for each shell ϕ and for all five liquids. Shells are defined by (a) RAD and (b) GC. Circle weightings indicate the probability of each point. U depends on N_1 for all liquids. The trends are very similar for each shell, justifying the averaging in Supplementary Figures S3 and S4.



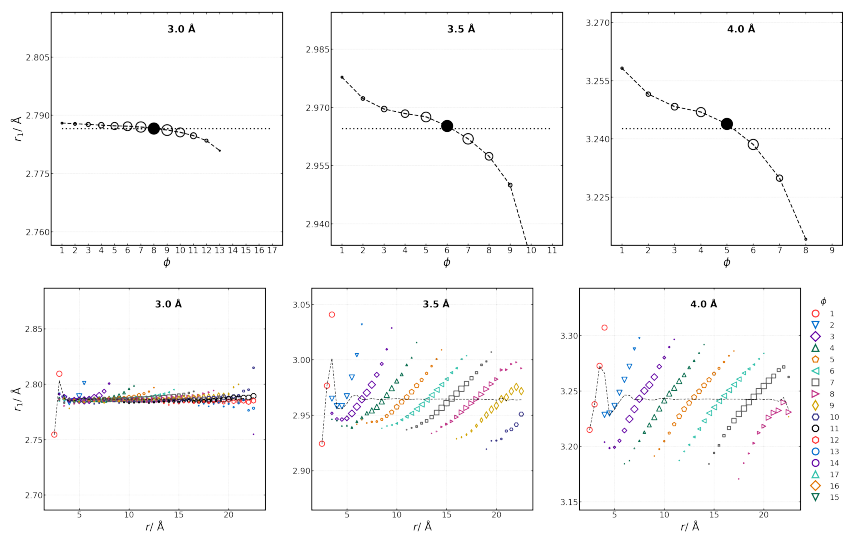
Supplementary Figure S9. Molecular potential energy U and molecular distance r for each coordination number N_1 and each shell index ϕ for all five liquids using (a) RAD and (b) GC. Circles are joined with dashed lines to represent a shared shell index ϕ . For all liquids, molecules with larger N_1 are found slightly further within each shell. This is a simpler version of Supplementary Figure S9, here emphasising the average U and average r in each shell.



Supplementary Figure S10. Average r_1 (black) and r_1 of each shell (colored by shell index ϕ and markers weighted by population) versus r using (a) RAD and (b) GC and a 0.5 Å bin width. There is an increasing dependence for all shells, all liquids and both methods.



Supplementary Figure S11. Molecular potential energy U of liquid water versus shell index ϕ for RAD in simulation boxes with lengths of 24, 40, 60 and 90 Å. The largest shell in each system is colored as a black circle. U does not converge to the bulk value (dotted black line) for the outermost shells but the deviation is smaller for larger boxes.



Supplementary Figure S12. Coordination radius r_1 versus versus shell index ϕ (top) and distance r (bottom) for three different GC cutoffs (3, 3.5 and 4 Å) for liquid water. Larger cutoffs bring about a greater variation in r_1 , suggesting that a smaller cutoff helps remove the variation in r_1 .